Available online at www.sciencedirect.com
SCIENCE DIRECT®
ELSEVIER
Journal of Constructional Steel Research 60 (2004) 161–182
JOURNAL OF CONSTRUCTIONAL STEEL RESEARCH
www.elsevier.com/locate/jcsr

Effect of cyclic thermal loading on the performance of steel H-piles in integral bridges with stub-abutments

Murat Dicleli *, Suhail M. Albhaisi

Department of Civil Engineering and Construction, Bradley University, 1501 West Bradley Avenue, Peoria, IL 61625, USA

Received 22 April 2003; received in revised form 21 August 2003; accepted 8 September 2003

Abstract

In this paper, analytical equations are developed to estimate the lateral displacement capacity of steel-H piles in integral bridges with stub abutments subjected to cyclic thermal variations. First, steel H piles that are capable of sustaining large plastic deformations are identified based on their local buckling strength. The normalized moment–curvature relationships of these piles are then obtained for various axial load levels. Next, a low-cycle fatigue damage model is employed to determine the maximum cyclic curvatures that such piles can sustain. The obtained moment–curvature relationships and cyclic curvature limits are used in static pushover analyses of two steel H-piles driven in soil to obtain the maximum thermal-induced cyclic lateral displacements such piles can sustain. Using the pushover analyses results, the displacement capacity of steel H-piles are formulated as a function of pile's properties, soil type and stiffness. Based on the obtained pile cyclic displacement capacities, the maximum length limits for integral bridges subjected to cyclic thermal variations are calculated. It is found that the maximum length limit for concrete integral bridges ranges between 150 and 265 m in cold climates and 180 and 320 m in moderate climates and that for steel integral bridges range between 80 and 145 m in cold climates and 125 and 220 m in moderate climates.

Keywords: Integral bridge; H-pile; Low-cycle fatigue; Inelastic behavior; Thermal displacement; Soil–pile interaction; Maximum length

* Corresponding author. Tel.: +1-309-677-3671; fax: +1-309-677-2867.
E-mail address: mdicleli@bradley.edu (M. Dicleli).

0143-974X/$ - see front matter © 2003 Elsevier Ltd. All rights reserved.
doi:10.1016/j.jcsr.2003.09.003

1. Introduction

Integral bridges possess a continuous deck and a movement system composed primarily of stub abutments supported on a single-row of flexible piles as illustrated in Fig. 1. In these types of bridges, the road surfaces are continuous from one approach embankment to the other and the abutments are cast integral with the piles, girders and the deck slab. The most common type of piles used at the abutments are steel H-piles.

The seasonal and daily temperature changes result in imposition of cyclic horizontal displacements on the continuous bridge deck of integral bridges and thus on the steel H-piles supporting the abutments. The magnitude of these cyclic displacements is a function of the temperature difference, the length and type of the bridge. As the length of integral bridges increases, the temperature-induced lateral cyclic displacements in the steel H-piles become larger as well. As a result, the piles may experience cyclic plastic deformations. This may result in the reduction of their service life due to low-cycle fatigue effects. Thus, the lengths of integral bridges should be limited to minimize such detrimental effects.

Currently, universal guidelines to determine the maximum length of integral bridges do not exist. Generally, bridge engineers depend on the performance of previously constructed integral bridges to specify the maximum lengths for their new designs. In 1982 [1], a study of integral bridge lengths in the USA revealed that continuous steel bridges with integral abutments have performed successfully for years in the 91 m range in North Dakota, South Dakota, and Tennessee and continuous concrete integral bridges, in the range of 152–183 m long have been constructed in Kansas, California, Colorado, and Tennessee. For years, bridge design engineers have depended on such crude data to determine the maximum length of integral bridges. Therefore, a rational guideline to determine the maximum length of integral bridges is urgently needed.

In this research, analytical equations are developed to estimate the lateral displacement capacity of steel-H piles in integral bridges with stub abutments subjected to cyclic thermal variations. First, steel H pile sections that are capable of sustaining large plastic deformations are identified based on their local buckling strength. The normalized moment–curvature relationships of these piles are then

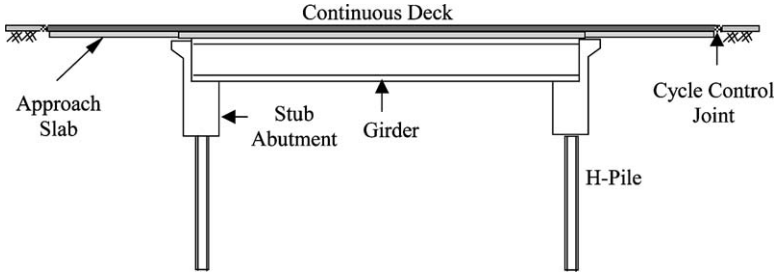

Fig. 1. Typical integral bridge with stub abutments.

obtained for various axial load levels. Next, a low-cycle fatigue damage model is employed to determine the maximum cyclic curvatures that such piles can sustain. The obtained moment–curvature relationships and cyclic curvature limits are used in static pushover analyses of two steel H-piles driven in soil to obtain the maximum thermal-induced cyclic lateral displacements such piles can sustain. Using the pushover analyses results, the displacement capacity of steel H-piles are formulated as a function of pile's properties, soil type and stiffness. The maximum length limits of concrete and steel integral bridges are then formulated as a function of the cyclic displacement capacity of steel H-piles.

It is noteworthy that the steel H-piles are assumed to be bearing on rock to avoid any interaction between their lateral movement and vertical frictional resistance, have adequate shear capacity, as is normally the case in most steel members [2] and adequate length to allow for inelastic moments to develop along the pile before the lateral soil strength is completely mobilized. This also ensures that the ultimate founding of the piles on rock is of no importance if they have adequate length to allow for inelastic moments to develop. A fixed connection is assumed between the piles and the abutment. As the integral bridges considered in this study are assumed to have stub-abutments, the shear and flexural failure of the abutments due to the effect of passive backfill pressure under positive temperature variations is not anticipated [3].

2. Plastic deformation capacity of H-piles

The lateral deformation capacity of steel members is affected by their buckling instability. The full scale tests on integral abutment bridge piles driven in stiff (virgin red clay) and loose soil (compacted fill material) have revealed that the piles are able to reach their plastic capacity with no buckling [4]. Thus, lateral–torsional or global buckling instabilities are not of concern. However, the width to thickness ratios of the flanges and the web for steel H-piles must be limited to allow for large plastic deformations without local buckling. In this study, the web–flange interaction approach presented by Kato [5] is used to calculate the local buckling strength of steel HP-sections commonly used as piles. Only the HP-sections commercially available in North America are considered.

Kato [5] defined the local buckling strength of an HP-section considering the interaction between the restraint provided by the web and flanges. Using a total of 68 test data on stub-columns made of HP sections, Kato [5] developed the following linear regression formula to relate the maximum stress, σ_u, that an HP section can undergo without local buckling, to the yield stress, σ_y, of the material:

$$\frac{\sigma_u}{\sigma_y} = \frac{1}{0.6003 + \dfrac{1.600}{\alpha_f} + \dfrac{0.1535}{\alpha_w}} \tag{1}$$

where α_f and α_w are the slenderness parameters for the flange and web, respectively. The slenderness parameters, α_f and α_w are defined as functions of the

geometric and material properties of the HP-sections as follows:

$$\alpha_f = \frac{E}{\alpha_y}\left(\frac{t_f}{b_f/2}\right)^2 \tag{2}$$

$$\alpha_y = \frac{E}{\alpha_y}\left(\frac{t_w}{d_w}\right)^2 \tag{3}$$

where, E is the Young's modulus, b_f is the flange width, d_w is the clear height of the web plate between flanges and t_f and t_w are, respectively, the flange and web thickness.

Table 1 displays the σ_u/σ_y values for HP sections made of ASTM A36, A572 grade 42 and 50 steels, which are the usual material specifications for HP sections available in North America. In the table, six out of the 11 HP-sections have σ_u/σ_y values larger than one for piles with A572-Grade 50 and 42 steels and nine HP-sections have σ_u/σ_y values larger than one for A36 steel. These sections are anticipated to develop stresses exceeding their yielding stress and may sustain considerable deformations before local buckling occurs. Only those piles, which do not exhibit any local buckling before yielding, are further studied.

3. Normalized moment curvature relationships of H-piles

As the relative rotation or displacement capacity of a steel member is proportional to its curvature capacity, the moment–curvature relationships of steel H-piles subjected to different levels of axial loads are obtained. The obtained moment–curvature relationships are then used to estimate the displacement capacity of steel H-piles under cyclic loading.

Fig. 2 displays the typical normalized moment–curvature relationships for those HP sections capable of sustaining large plastic deformations and subjected to an axial load equal to 30% of their axial yield capacity, P_y. The normalized moment–curvature relationships are obtained by dividing the moment by the yield moment, M_y and the curvature by the yield curvature, Φ_y. As observed from the figure, the normalized relationships are identical for all the piles bending about their strong axis. Similar observations are made for the same piles bending about their weak axis.

Fig. 3 displays typical normalized moment–curvature relationships for an HP250X85 section. The curves are presented for two different axial loads equal to 30 and 60% of the pile's axial yield capacity and ASTM A36 and A572-G50 steels. It is observed that for axial load levels larger than 10% of the yield axial load, the normalized moment–curvature relationships are nearly identical up to the strain hardening point even for different steel grades [3].

Table 1
The ratios of buckling to yield stress for HP-sections and different steel grades

Pile size	A36			A570-G42			A570-G50		
	σ_u/σ_y	σ_y (MPa)	σ_u (MPa)	σ_u/σ_y	σ_y (MPa)	σ_u (MPa)	σ_u/σ_y	σ_y (MPa)	σ_u (MPa)
HP360x174	1.22	248	303	1.17	289	339	1.11	344	382
HP360x152	1.14	248	282	1.08	289	312	1.01	344	348
HP360x132	1.04	248	257	0.98	289	282	0.90	344	310
HP360x108	0.88	248	218	0.82	289	236	0.74	344	256
HP310x125	1.24	248	307	1.19	289	343	1.13	344	387
HP310x110	1.16	248	289	1.11	289	321	1.04	344	359
HP310x94	1.04	248	258	0.98	289	284	0.91	344	313
HP310x79	0.91	248	224	0.84	289	243	0.77	344	265
HP250x85	1.24	248	307	1.19	289	343	1.10	344	387
HP250x62	1.03	248	256	0.97	289	281	0.90	344	310
HP200x63	1.23	248	304	1.17	289	339	1.11	344	383

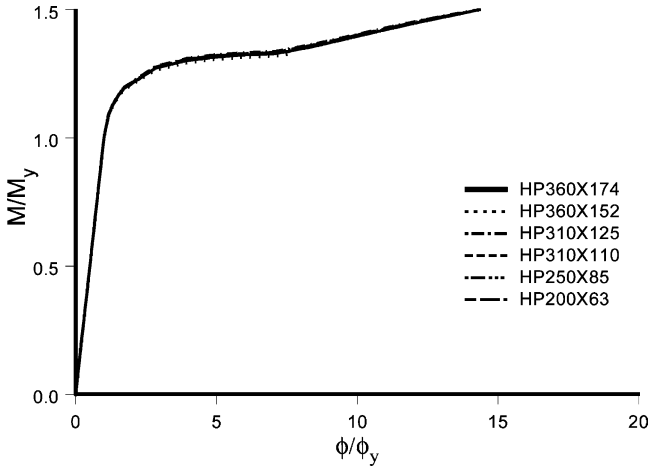

Fig. 2. Normalized MCR for all sections under $0.3P_y$ axial load (A572-G50, strong axis bending).

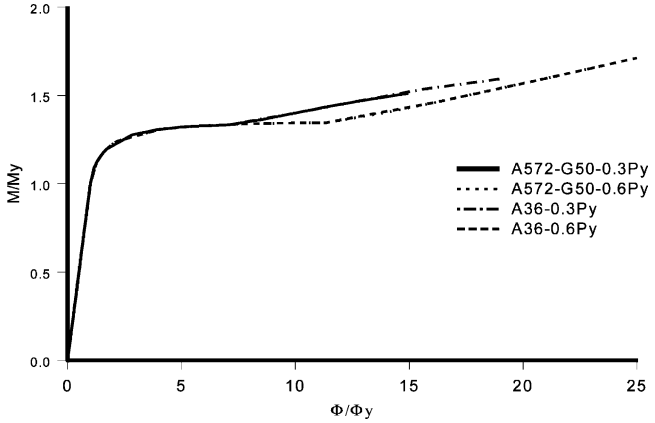

Fig. 3. Normalized MCR for HP250X85 under 0.3 P_Y and 0.6 P_y axial loads (A572-G50, A36, strong axis bending).

4. Cyclic thermal-induced strains in H-piles

The thermal-induced longitudinal movement of the integral bridge deck results in one dominant cyclic lateral displacement of steel H-piles at the abutments each year due to seasonal (summer and winter) temperature changes and numerous smaller cyclic lateral displacements due to daily and/or weekly temperature fluctuations. This is confirmed by the research studies of England and Tsang [6] and by the strain vs. time records of instrumented steel H-piles for two integral bridges in the state of Iowa [7]. The instrumented piles of both bridges in the state of Iowa

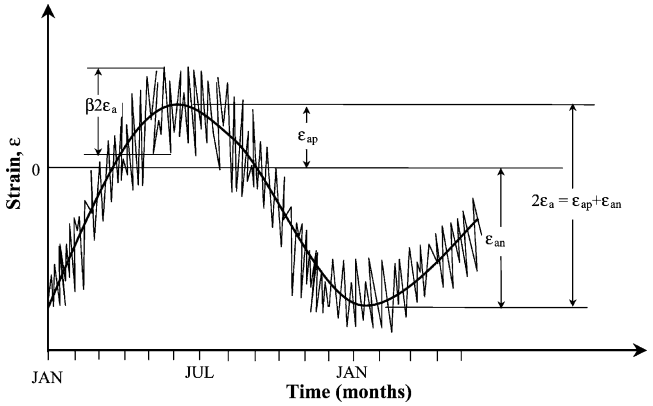

Fig. 4. Variation of pile strain as a function of time in integral bridges.

exhibited one large strain cycle per year due to seasonal temperature changes and about 52 small, but noticeable, strain cycles per year as qualitatively illustrated in Fig. 3. Moreover, the field-test records demonstrated that the amplitude of the small strain cycles in the piles fall within 20 to 40% range of the amplitude of the large strain cycles. The above observations are assumed to be generally applicable to integral bridges in North America in lieu of extensive field test data.

It is noteworthy that the net difference between the seasonal and reference (construction) temperatures may be disparate in the summer and winter times based on the climatic conditions of the area where the bridge is located. Therefore, the amplitudes of the positive (ε_{ap}) and negative (ε_{an}) strain cycles corresponding to the summer and winter times may not be equal as observed from Fig. 4. However, as the range of strain amplitudes rather than the strain amplitude itself defines the extent of fatigue damage in steel H-piles, the positive and negative strain amplitudes are assumed to be equal for the purpose of this study.

5. Thermal-induced low-cycle fatigue effects in steel H-piles

Low-cycle fatigue failure of structural components is caused by cyclic loads or displacements of relatively larger magnitude that may produce significant amounts of plastic strains in the structural component. Generally, the number of displacement cycles that leads to failure of a component is determined as a function of the plastic strains in the localized region of the component being analyzed. This is referred to as strain-based approach to fatigue life estimate of structural components. This approach is appropriate for determining the fatigue life of steel H-piles supporting the abutments as it considers the temperature-induced large plastic deformations that may occur in localized regions of the piles where fatigue cracks may begin.

Koh and Stephens [8] proposed an equation to calculate the number of constant amplitude strain cycles to failure for steel sections under low cycle fatigue. This equation is based on the total strain amplitude, ε_a, and expressed as follows:

$$\varepsilon_a = M\left(2N_f\right)^m \tag{4}$$

where $M = 0.0795$, $m = -0.448$ and N_f is the number of cycles to failure. The above equation is used for the estimation of the maximum strain amplitude steel H-piles can sustain before their failure takes place due to low-cycle fatigue effects within the service life of the bridge.

For a bridge to serve its intended purpose, it must sustain the effect of temperature-induced cyclic displacements throughout its service life. The temperature-induced strains in steel H-piles are assumed to have variable amplitudes consisting of large and small cycles as illustrated in Fig. 4. Therefore, Eq. (4), which is derived for constant amplitude cycles, cannot be used directly to obtain the maximum strain amplitude a pile may sustain. Conservatively assuming that both the large and small cycles induce low cycle fatigue damage in the steel H-piles, Miner's rule [9] may be used in combination with Eq. (4) to obtain the maximum strain amplitude a pile may sustain.

Miner [9] defined the cumulative fatigue damage induced in a structural member by load or displacement cycles of different amplitudes as:

$$\sum_{i=1}^{n} \frac{n_i}{N_i} \leq 1 \tag{5}$$

where, n_i is the cycles associated with the ith loading (or displacement) case and N_i is the number of cycles to failure for the same case. The above equation states that if a load or displacement is applied n_i times, only a fraction, n_i/N_i of the fatigue life has been consumed. The fatigue failure is then assumed to take place when n_i/N_i ratios of the cycles with different amplitudes add up to 1.

Applying Miner's rule to the small and large amplitude pile strains, the following expression is obtained:

$$\frac{n_s}{N_{fs}} + \frac{n_l}{N_{fl}} = 1 \tag{6}$$

where, n_s and n_l are, respectively, the number of small and large amplitude strain cycles due to temperature variations throughout the service life of the bridge, and N_{fs} and N_{fl} are the total number of cycles to failure for the corresponding small and the large amplitude strain cycles, respectively. For a bridge with 'n' years of service life, the number of small-amplitude cycles are $n_s = 52\,n$ and the number of large amplitude cycles are $n_l = n$. Using Eq. (4), the small and large amplitude strains are then expressed as:

$$\varepsilon_{as} = M\left(2N_{fs}\right)^m \tag{7}$$

$$\varepsilon_{al} = M\left(2N_{fl}\right)^m. \tag{8}$$

The small strain amplitude, ε_{as}, may be expressed as a fraction of the large strain amplitude, ε_{al}, as follows (Fig. 4):

$$\varepsilon_{as} = \beta * \varepsilon_{al} \tag{9}$$

where β is a positive constant smaller than one. Substituting Eq. (9) into Eq. (7) and solving for N_{fs} and N_{fl}, the numbers of small and large amplitude cycles to failure are obtained as follows;

$$N_{fs} = \frac{1}{2}\left(\frac{\beta * \varepsilon_{al}}{M}\right)^{\frac{1}{m}} \tag{10}$$

$$N_{fl} = \frac{1}{2}\left(\frac{\varepsilon_{al}}{M}\right)^{\frac{1}{m}} \tag{11}$$

Substituting Eqs. (10) and (11) into Eq. (6) and solving for ε_{al}, the maximum large amplitude strain a pile may sustain is then obtained as:

$$\varepsilon_{al} = \left(\frac{2n_s}{\left(\frac{\beta}{M}\right)^{\frac{1}{m}}} + \frac{2n_l}{\left(\frac{1}{M}\right)^{\frac{1}{m}}}\right)^{m} \tag{12}$$

To estimate the maximum strain amplitude a steel pile can sustain, a service life of 75 years is assumed for integral bridges per AASHTO bridge design specifications [10]. Table 2 tabulates the values of maximum large and small amplitude strains for different values of βs. The values of small strain amplitude, ε_{as}, range from 0.00113 for $\beta = 0.2$ to 0.00135 for $\beta = 0.4$. For steel grades of A36 and A570-G50, the yield strain, ε_y, is 0.0125 and 0.00175, respectively. This indicates that the value of ε_{as} is less than the yielding strain for some range of large strain amplitude, ε_{al}, values. However, considering the fact that most of the small cycles occur while the pile has already yielded [11], the small amplitude cycle may result in further plastic deformation of the pile as illustrated in Fig. 5. Thus, this may justify the initial low cycle fatigue effect assumption for the small cycles. For this reason, the small amplitude strain cycles are conservatively assumed to result in low cycle

Table 2
Values of ε_{al} and ε_{as} for different β values and service life of bridges

Service life (years)	ε_{as}			ε_{al}		
	β			β		
	0.2	0.3	0.4	0.2	0.3	0.4
50	0.001357	0.001539	0.001617	0.006784	0.005657	0.004973
75	0.001131	0.001283	0.001348	0.005129	0.004277	0.00376
100	0.000995	0.001128	0.001185	0.004042	0.00337	0.002963

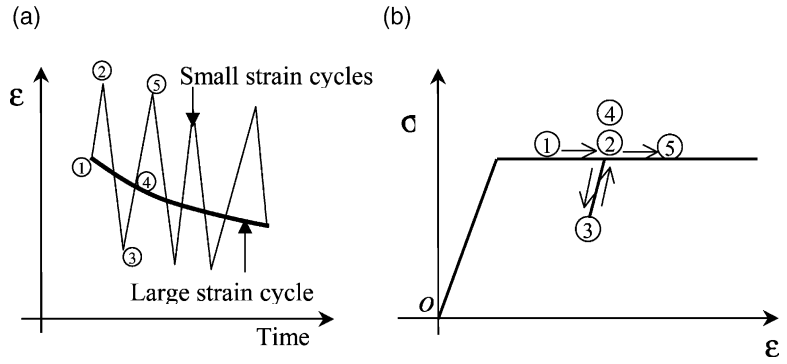

Fig. 5. Loading and unloading due to small cycles (a) strain vs. time; (b) stress vs. strain.

fatigue. Accordingly, for an average value of $\beta = 0.3$, the maximum strain amplitude that the piles can sustain is obtained as 0.004277 from Table 2.

Using the calculated maximum large strain amplitude, $\varepsilon_{al} = 0.004277$, the maximum cyclic curvature amplitude, Φ_f, at fatigue failure of the pile is expressed as [3]:

$$\Phi_f = \frac{2\varepsilon_{al}}{d_p} = \frac{0.0085}{d_p} \tag{13}$$

where, d_p is the width of the pile in the direction of the cyclic displacement. The cyclic moment amplitude, M_f, corresponding to the calculated curvature amplitude, Φ_f, at fatigue failure of the pile is then obtained from the pile's normalized moment–curvature diagram. This moment is used as a control flag to determine the displacement capacity of the steel H-piles using the static pushover analyses results.

6. Steel H-piles and soil types considered in the study

A parametric study is conducted to investigate the effects of pile and foundation soil properties on the displacement capacity of steel H-piles and hence on the displacement capacity of integral bridges with stub-abutments subjected to cyclic temperature variations. The results of the parametric study are then used to obtain analytical expressions to determine the cyclic displacement capacity of steel H-piles and the maximum length limits of integral bridges with stub abutments as a function of the pile and foundation soil properties.

The stiffness of the piles and the foundation soil is anticipated to affect the displacement capacity of integral bridges. Thus, two different pile sizes, HP250X85 and HP310X125 are included in the parametric study. The selected piles have a superior ductility capacity as observed from Table 1 and cover a wide range of H-pile sizes used by many departments of transportation in North America. Furthermore, the piles are assumed to be made of ASTM A36 steel, which is the usual material specification for steel H-piles used in North America. Orientation of the piles for

bending about their strong and weak axes is also considered in the parametric study. Moreover, the abutment–pile connection detail is believed to have a significant effect on the pile stresses [12]. Accordingly, in addition to fixed connection detail between the pile and the abutment, a pin connection detail is also included in the parametric study. The foundation soil is assumed to be either clay or sand. Four different sand and clay stiffnesses are included in the study.

7. Soil–H-pile interaction behavior

The soil–pile interaction for a particular point along the pile is defined by a non-linear load (P)-deformation (Y) curve or P–Y curve, where P is the lateral soil resistance per unit length of pile and Y is the lateral deflection. The computation of the lateral-force–displacement response of a pile involves the construction of a full set of P–Y curves along the pile to model the force–deformation response of the soil. A typical P–Y curve for soil subjected to lateral movement of a pile is shown with a solid line in Fig. 6. This non-linear behavior may be simplified using an elasto-plastic curve displayed on the same figure with a dashed line. The elastic portion is defined with a slope equal to the secant soil modulus, E_s, for clay and initial soil modulus, E_s, for sand and the plastic portion is defined as the ultimate soil resistance per unit length of pile, P_u [13].

7.1. Piles driven in clay

For piles driven in clay the ultimate soil resistance per unit length of pile, P_u, is expressed as [13]:

$$P_u = 9C_u d_p \tag{14}$$

where C_u is the undrained shear strength of the clay and d_p is the pile width.

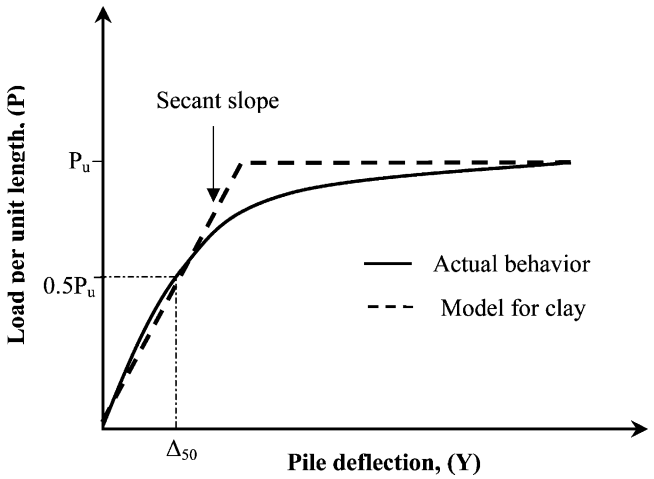

Fig. 6. Actual and modeled P–Y curve.

Based on the method proposed by Skempton [14], the elastic soil modulus, E_s, for clay is obtained as:

$$E_s = \frac{9C_u}{5\varepsilon_{50}} \tag{15}$$

where ε_{50} is the soil strain at 50% of ultimate soil resistance.

For soft, medium, medium-stiff and stiff clay, corresponding values of $C_u = 20$, 40, 80 and 120 kPa [15] and $\varepsilon_{50} = 0.02$, 0.01, 0.0065 and 0.0050 [16] are used in the parametric study.

7.2. Piles driven in sand

For piles driven in sand, the ultimate soil resistance per unit length of pile, P_u, is expressed as [13]:

$$P_u = k_a d_p(\gamma x + q)\left(\tan^8\beta - 1\right) + k_0 d_p(\gamma x + q)\tan^4\beta\tan\phi \tag{16}$$

where k_a and k_o are, respectively, the active and at-rest earth pressure coefficients; γ and ϕ are, respectively, the unit weight and the angle of internal friction of the soil in degrees, x is the depth below the ground surface, q is the surcharge pressure and β is expressed as:

$$\beta = \left(45 + \frac{\phi}{2}\right) \tag{17}$$

For sand, E_s is assumed to increase linearly with depth from the ground surface and is expressed as [13]:

$$E_s = kx \tag{18}$$

where k is the subgrade constant of the soil.

For loose, medium, medium-dense and dense sand, corresponding values of $k = 2000$, 6000, 8000 and 12000 kN/m^3, $\gamma = 16$, 18, 19 and 20 kN /m^3 and $\phi = 30^\circ$, 35°, 37.5° and 40° are used in the parametric study [15].

8. Structural model for pushover analysis of the pile–soil system

Static pushover analyses of the two aforementioned H-piles are conducted to estimate their cyclic displacement capacity based on the fatigue curvature limit expressed by Eq. (13). For this purpose, nonlinear structural model of the piles incorporating the response of the soil to bridge movement are built using the finite element-based software SAP2000 [17]. The pile–soil model is illustrated in Fig. 7. In the model, the length of the pile effective in responding to the lateral temperature-induced loads and displacements is taken as 30 times the pile width. The portion of the pile below this length is believed to have negligible effect on the pile–soil interaction behavior as the lateral movements of the piles at such depths are insignificant [18]. This also ensures that the initial assumption related to the ultimate founding of the pile on rock is of no importance if it has a length equal to 30

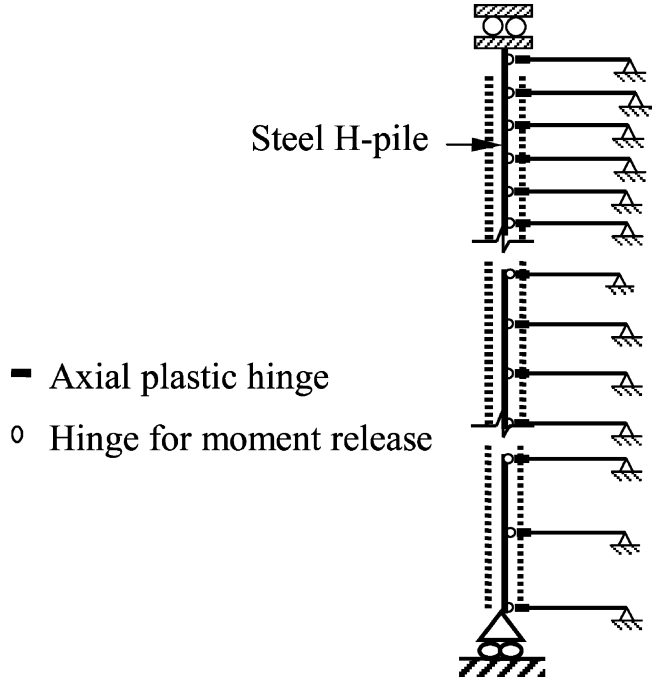

Fig. 7. Nonlinear structural model.

times the pile width. The pile is modeled using beam elements with nonlinear frame-hinges to simulate the inelastic deformation of the steel H-piles under thermal effects. It is noteworthy that the presence of the backfill behind the abutments is observed to slightly enhance the cyclic displacement capacity of the steel H-piles and therefore its effect is not considered in the static pushover analyses of the piles [3]. Furthermore, the pile top is conservatively assumed as fixed due to the large stiffness of the deck and the stub abutment relative to that of the pile. However, when studying the effect of pinned pile-abutment connection on the cyclic displacement capacity of the pile, a hinge is introduced at the pile top to allow for rotation.

Horizontal truss elements with plastic axial hinges at their ends are attached at each node along the pile to model the nonlinear force–deformation behavior of the soil as shown in Fig. 7. The lateral soil reactions are usually concentrated along the top 5 to 10 pile diameters [18]. Accordingly, for the top 2 m of the pile, the nodes are closely spaced (0.1 m) to accurately model the behavior of the soil. The spacing of the nodes is then gradually increased in steps along the length of the pile. A roller support is assigned at the bottom of the end-bearing pile to provide stability in the vertical direction.

In the model, the force–deformation (P–Y) behavior of the soil is defined by the yield force, F_{ty}, of the plastic axial hinge introduced at the end of each truss element and the elastic stiffness, K_t, of the truss element. The yield force, F_{ty}, is

calculated by multiplying the ultimate soil resistance per unit length, P_u, by the tributary length, h_t, between the nodes along the pile. Thus

$$F_y = P_u h_t \tag{19}$$

Similarly, the elastic stiffness of the truss element is calculated by multiplying the soil modulus by the tributary length, h_t, between the nodes along the pile:

$$K_t = E_s h_t \tag{20}$$

9. Static pushover analyses results

A total of 64 static pushover analyses are conducted to estimate the displacement capacity of steel H-piles under cyclic thermal loading. In the analyses, the piles are assumed to carry a typical axial dead load equal to 30% of their axial capacity. Accordingly, the moment–curvature relationship of the piles for the aforementioned axial load level is used to define the nonlinear hinge properties of the pile elements and the moment at fatigue failure. The analyses results are presented in Table 3 for clay and Table 4 for sand. In the following subsections the effect of various structural and geotechnical parameters on the displacement capacity of steel H-piles is studied using the available analysis results.

9.1. Foundation soil stiffness

The stiffness of the foundation soil is observed to have a remarkable effect on the maximum temperature-induced displacement, Δ_P, that a steel H-pile can accommodate. As the soil stiffness increases, the displacement capacity of the piles and hence that of integral bridges decreases as observed from Tables 3 and 4. For example, the ratio of the displacement capacities of the same pile driven in loose and dense sand ranges between 2.3 to 2.7, depending on the pile size and orientation.

Table 3
Displacement capacity of H-piles driven in clay for fixed and pinned pile-abutment connection

Pile connection fixity	C_u (KPa)	HP310X125		HP250X85	
		Strong axis Δ_P (m)	Weak axis Δ_P (m)	Strong axis Δ_P (m)	Weak axis Δ_P (m)
Fixed	20	0.105	0.118	0.082	0.095
	40	0.051	0.053	0.039	0.044
	80	0.027	0.026	0.021	0.020
	120	0.020	0.017	0.015	0.013
Pinned	20	0.632	0.708	0.451	0.577
	40	0.280	0.331	0.219	0.264
	80	0.137	0.165	0.116	0.131
	120	0.091	0.105	0.078	0.081

Table 4
Displacement capacity of H-piles driven in sand for fixed and pinned pile-abutment connection

Pile connection fixity	k (KN/m^3)	HP310X125		HP250X85	
		Strong axis Δ_P (m)	Weak axis Δ_P (m)	Strong axis Δ_P (m)	Weak axis Δ_P (m)
Fixed	2000	0.057	0.059	0.044	0.053
	6000	0.038	0.040	0.030	0.031
	12000	0.027	0.029	0.022	0.023
	18000	0.023	0.025	0.019	0.020
Pinned	2000	0.173	0.227	0.158	0.194
	6000	0.113	0.146	0.099	0.122
	12000	0.085	0.105	0.072	0.085
	18000	0.071	0.083	0.060	0.067

9.2. Pile size and orientation

The results presented in Tables 3 and 4 clearly reveal that as the size of the pile increases, its displacement capacity increases. The greater bending capacity of larger piles requires larger displacements to reach the fatigue curvature limit. This allows for larger cyclic displacements before fatigue failure of the piles takes place.

The effect of pile orientation on the displacement capacity of the integral bridges with stub abutments is displayed in Tables 3 and 4. The analyses results revealed that the axis of bending has only a negligible effect on the displacement capacity of integral bridges with stub abutments. This may not be true for bridges with larger abutment height [3].

9.3. Pile–abutment connection type

A pinned abutment–pile connection dramatically increases the cyclic displacement capacity of the piles as observed from the results presented in Tables 3 and 4. For loose sand, the pile's displacement capacity for the pinned case is about three times that for the fixed case. The difference is almost the same for dense sand. For soft clay, the pile's displacement capacity for the pinned case is about six times that for the fixed case. The difference is reduced to about four times for stiff clay.

9.4. Formulation of cyclic displacement capacity of steel H-piles

In this section, the development of analytical tools to estimate the cyclic displacement capacity of steel H-piles based on the pushover analyses results, is presented. To formulate the displacement capacity, Δ_p, of a steel H-pile as a function of soil and pile properties, the pile is idealized as an equivalent cantilever with a theoretical equivalent displacement length, l_{ed}, as illustrated in Fig. 8. This equivalent displacement length, l_{ed}, is assumed to be proportional to the pile's critical length, l_c by a factor, λ. Thus

$$l_{ed} = \lambda l_c \tag{21}$$

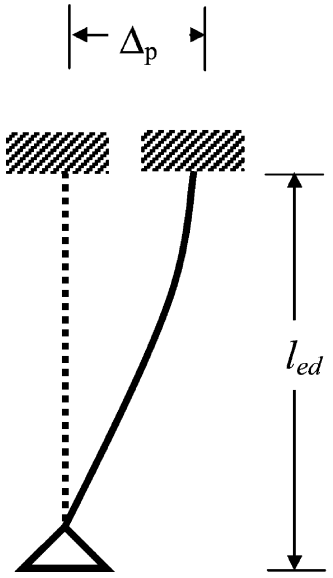

Fig. 8. The effective displacement length, l_{ed}.

The pile's critical length, l_c, is defined as the depth below which the displacements and bending moments at the pile head have little effect and it is calculated as follows [7]:

$$l_c = 4\sqrt[4]{\frac{E_p I_p}{k_h}} \tag{22}$$

where E_p is the pile's modulus of elasticity, I_p is the pile's moment of inertia, and k_h is the initial soil lateral stiffness. Table 5 summarizes the expressions for k_h for clay and sand. In the table, x represents the distance measured from the pile top and is set equal to the distance from the pile top to the middle of the critical length, where the soil stiffness can be averaged [7]. For that reason, an iterative analysis procedure is followed to calculate the value of x. For the static pushover cases studied, the iterative analysis resulted in an x value between 6 and 10 times the pile width, d_p. Accordingly an average value of $8d_p$ is assumed for x.

Table 5
Initial soil stiffness, k_h, [7]

Soil type	k_h
Soft clay and stiff clay	$\frac{9C_u}{2.5\varepsilon_{50}}$
Very stiff clay	$\frac{9C_u}{4\varepsilon_{50}}$
Sand	kx

At fatigue failure, the maximum cyclic moment at the fixed end of the equivalent cantilever is set equal to M_f (cyclic moment at fatigue failure) as illustrated in Fig. 9. The moment distribution along this equivalent cantilever is assumed to be linear. The curvature variation corresponding to this linear moment distribution along the equivalent cantilever is also illustrated in Fig. 9. Note that the variation of the curvature between the curvature at yield, ϕ_y, and the curvature at fatigue failure, ϕ_f, is approximated by a linear line.

The displacement, Δ_p, of the pile, is then obtained by taking the moment of the area under the curvature diagram of Fig. 9 about the free end of the equivalent cantilever. Thus

$$\Delta_p = \frac{\phi_y(\lambda l_c)^2}{6}\left(1+\frac{M_y}{M_f}\right)+\frac{\phi_f(\lambda l_c)^2}{6}\left(2-\frac{M_y}{M_f}-\left(\frac{M_y}{M_f}\right)^2\right) \tag{23}$$

The factor λ is obtained by setting, Δ_p, of Eq. (23) equal to the pile's displacement obtained from the static pushover analyses results for clay and sand. Table 6 summarizes the values of λ for different soil and abutment–pile connections. Tables 7 and 8 display comparison of the pushover analysis results for pile displacement limits with those obtained using Eq. (23), respectively, for clay and sand. The results presented in Tables 7 and 8 show a reasonably good agreement.

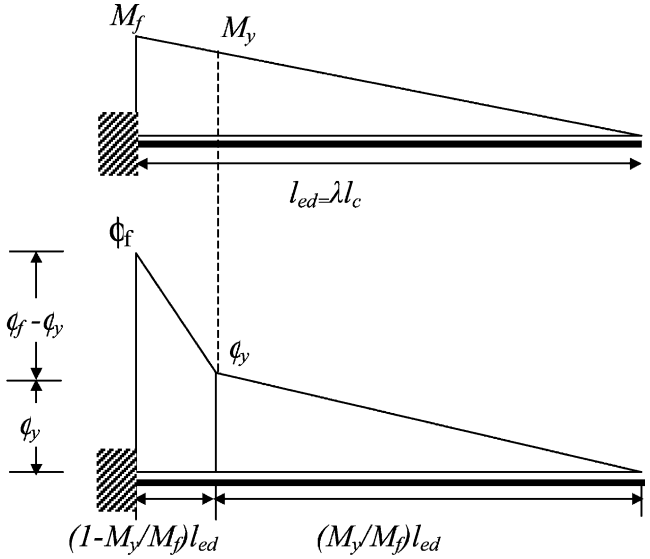

Fig. 9. Moment distribution along the idealized pile.

Table 6
λ values for different soil and abutment-pile connections types

Soil	Abutment–pile connection	Strong axis	Weak axis
Clay	Fixed	0.5	0.55
	Pinned	1.15	1.40
Sand	Fixed	0.65	0.75
	Pinned	1.1	1.40

Table 7
Comparison of static pushover analysis results and Eq. (23) for piles driven in clay and bending about their strong axis

Pile connection fixity	C_u (Kpa)	HP310X125		HP250X85	
		Eq. (23) Δ_P (m)	Pushover analyses Δ_P (m)	Eq. (23) Δ_P (m)	Pushover analyses Δ_P (m)
Fixed	20	0.095	0.105	0.081	0.082
	40	0.053	0.051	0.041	0.039
	80	0.027	0.027	0.023	0.021
	120	0.019	0.020	0.017	0.015
Pinned	20	0.501	0.532	0.428	0.451
	40	0.282	0.280	0.215	0.219
	80	0.143	0.137	0.121	0.116
	120	0.103	0.091	0.088	0.078

Table 8
Comparison of static pushover analysis results and Eq. (23) for piles driven in sand and bending about their strong axis

Pile connection fixity	k (KN/m^3)	HP310X125		HP250X85	
		Eq. (23) Δ_P (m)	Pushover analyses Δ_P (m)	Eq. (23) Δ_P (m)	Pushover analyses Δ_P (m)
Fixed	2000	0.065	0.057	0.049	0.044
	6000	0.037	0.038	0.028	0.030
	12000	0.026	0.027	0.020	0.022
	18000	0.022	0.023	0.016	0.019
Pinned	2000	0.186	0.173	0.165	0.158
	6000	0.107	0.113	0.095	0.099
	12000	0.076	0.085	0.067	0.072
	18000	0.062	0.071	0.055	0.060

10. Formulation of maximum length limits of integral bridges with stub abutments

The average thermal displacement at one end of the bridge deck is expressed as

$$\Delta_d = \gamma_T \alpha_T \Delta T \frac{L}{2} \tag{24}$$

where, γ_T is the load factor for thermal effects, which is specified as 1.2 by AASHTO [10], α_T is the coefficient of thermal expansion for the deck's material, ΔT is the average of the negative and positive thermal variation and L is the total length of the bridge. Setting up the above equation equal to the pile's displacement capacity, Δ_P, under cyclic thermal loading and solving for L, the maximum length limit of integral bridges with stub abutments is expressed as:

$$L = \frac{2}{\gamma_T \alpha_T \Delta T}\left[\frac{\phi_y(\lambda l_c)^2}{6}\left(1+\frac{M_y}{M_f}\right)+\frac{\phi_f(\lambda l_c)^2}{6}\left(2-\frac{M_y}{M_f}-\left(\frac{M_y}{M_f}\right)^2\right)\right] \tag{25}$$

To express the above equation in a more practical form, first, the moment at fatigue failure is approximated by conservatively setting it up equal to the plastic moment capacity, M_p, of the pile incorporating the effect of the axial load. Then, the pile's yield curvature is expressed as:

$$\phi_y = \frac{M_y}{E_p I_p} \tag{26}$$

where the yield moment M_y also incorporates the effect of the axial load. Substituting $M_f = M_p$, Eqs. (13) and (26) into Eq. (25), the maximum length limit of integral bridges with stub abutments, based on the displacement capacity of the piles under cyclic thermal loading is expressed as:

$$L := \frac{2}{\gamma_T \alpha_T \Delta T}\left[\frac{M_y(\lambda l_c)^2}{6E_p I_p}\left(1+\frac{M_y}{M_p}\right)+\frac{0.0085(\lambda l_c)^2}{6d_p}\left(2-\frac{M_y}{M_p}-\left(\frac{M_y}{M_p}\right)^2\right)\right] \tag{27}$$

AASHTO [10] specifies minimum and maximum temperatures for the design of bridges under thermal effects for moderate and cold climates. Assuming a construction temperature of 15 °C, and using the temperature ranges specified by AASHTO [10], the average temperature ranges for steel and concrete bridges are respectively calculated as 34° and 20° for moderate climates and as 43° and 23° for cold climates.

Table 9 presents the maximum length limits of steel and concrete integral bridges with stub abutments located in moderate and cold climates per AASHTO [10] definition. The data in the tables are obtained using the above equation applied to various steel H-pile sizes commonly used in practice. The piles are assumed to have fixed connection to the abutment as normally found in most integral bridges and be made of ASTM A36 steel, which is the usual material specification for steel

Table 9
Maximum length limits for steel and concrete integral bridges based on pile's displacement capacity

Pile size	Steel bridges		Concrete bridges	
	Moderate climate L (m)	Cold climate L (m)	Moderate climate L (m)	Cold climate L (m)
HP310x125	220	145	320	265
HP310x110	205	135	300	250
HP250x85	160	110	240	195
HP200x63	125	80	180	150

H-piles used in North America. Furthermore, for piles in stiff soil conditions, pre-drilled oversize holes filled with loose sand is generally provided along the top portion of the pile to reduce the resistance of the surrounding stiff soil to lateral movements of the pile. Accordingly, the length limits presented in Table 9 are obtained assuming medium-stiff clay.

The data presented in Table 9 revealed that the maximum length limit for concrete integral bridges ranges between 150 and 265 m in cold climates and 180 and 320 m in moderate climates and that for steel integral bridges range between 80 and 145 m in cold climates and 125 and 220 m in moderate climates for different pile sizes. It is noteworthy that the results from the full-scale tests at the University of Tennessee [19] on integral bridges resting on clay recommend length limits for integral bridges, which are based on an average 35-mm displacement limit for the piles at the abutments. This is in close agreement with the pile displacement limits for medium to medium-stiff clay, hence the integral bridge length limits proposed in this study.

The maximum length limits of integral bridges imposed by various state departments of transportation are presented in Table 10 for comparison purposes. The calculated maximum length limits are in close agreement with those proposed by Colorado and Tennessee departments of transportation. However, the rest of the state departments of transportation presented in Table 10 impose smaller maximum length limits in lieu of sufficient experimental and analytical research results on the behavior of integral bridges subjected to uniform temperature

Table 10
Maximum length limits for integral abutment bridges

Department of Transportation	Steel bridges (maximum length (m))	Concrete bridges (maximum length (m))
Colorado	195	240
Illinois	95	125
New Jersey	140	140
Ontario, Canada	100	100
Tennessee	152	244
Washington	91	107

variations. It is noteworthy that the Tennessee Department of Transportation has constructed a 360-m long concrete integral bridge. This length is longer than the 320-m upper length limit provided in Table 9 for concrete integral bridges in moderate climates. In Tennessee, the yield stress of steel for the H-piles used in integral bridges is generally 345 MPa (50 ksi). However, the maximum length limits presented in Table 9 are based on 248 MPa (36 ksi) yield stress. For 345 MPa yield stress, the upper length limit for integral bridges in moderate climates is calculated as 400 m using Eq. (27). This is longer than the length of the 360-m long bridge built in the state of Tennessee. This justifies the practical applicability of the proposed equation.

11. Conclusions

Followings are the conclusions drawn from this study:

- The cyclic displacement capacity of steel H-piles in integral bridges with stub abutments decreases considerably as the foundation soil becomes stiffer. Consequently, the maximum length limits for integral bridges with stub abutments also decrease as the foundation soil becomes stiffer.
- The effect of the orientation of the steel H-piles on the displacement capacity of integral bridges with stub abutments is negligible.
- It is found that a pinned abutment–pile connection dramatically increases the displacement capacity of integral bridges with stub abutments based on piles' displacement capacity under cyclic loading.
- Concrete bridges are more suited for integral bridge construction as they are less sensitive to temperature variations and are recommended especially in cold climates.
- Stub abutments are strongly recommended to eliminate the possibility of abutment's flexural failure.
- It is found that the maximum length limit for concrete integral bridges ranges between 150 and 265 m in cold climates and 180 and 320 m in moderate climates and that for steel integral bridges range between 80 and 145 m in cold climates and 125 and 220 m in moderate climates.

References

[1] Greimann LF, Abendtroth RE, Johnson DE, Ebner PB. Pile design and tests for integral-abutment bridges. Final report, Iowa Department of Transportation, Project HR-273, Ames, Iowa, USA, 1987.

[2] Dicleli M, Bruneau M. Quantitative approach to rapid seismic evaluation of slab-on-girder steel highway bridges. ASCE Journal of Structural Engineering 1996;122(10):1160–8.

[3] Dicleli M, Albhaisi SM. Maximum lengths of integral abutment bridges based on the strength of abutments and the performance of steel H-piles under cyclic thermal loading. BU-CEC-03-01, Department of Civil Engineering and Construction, Bradley University, Peoria, IL, 2003.

[4] Ingram EE, Burdette EG, Goodpasture DW, Deatherage JH. Evaluation of applicability of typical column design equations to steel H-piles supporting integral abutments. Engineering Journal 2003;First Quarter:50–8.
[5] Kato B. Rotation capacity of H-section members as determined by local buckling. Journal of Constructional Steel Research 1989;13(2–3):95–109.
[6] England GL, Tsang NCM. Towards the design of soil loading for integral bridges—experimental evaluation. Department of Civil and Environmental Engineering, Imperial College, London, 2001 http://www.concrete.cv.ic.ac.uk./research/Case/int-bridge/int-main.htm.
[7] Girton DD, Hawkinson TR, Greimann LF, Bergenson K, Ndon U, Abendorth RE. Validation of design recommendations for integral-abutment piles. Iowa Department of Transportation, Project HR-292, Ames, Iowa, USA, 1989.
[8] Koh SK, Stephens RI. Mean stress effects on low cycle fatigue for a high strength steel. Fatigue and Fracture of Engineering Materials and Structures 1991;14(4):413–28.
[9] Miner MA. Cumulative damage in fatigue. Journal of Applied Mechanics 1945;12.
[10] AASHTO LRFD Bridge Design Specifications, 2nd ed, Washington, DC, USA, 1998.
[11] Lawyer A, French C, Shield CK, Field performance of integral abutment bridge, Transportation Research Record, National Science Foundation, No 1740, 2000:108–117.
[12] Dicleli M. Simplified model for computer-aided analysis of integral bridges. ASCE Journal of Bridge Engineering 2000;5(3):240–8.
[13] Haliburton TA. Soil structure interaction; numerical analysis of beams and beam columns, Technical Publication No. 14, School of Civil Engineering, Oklahoma State University, Stillwater, Oklahoma, 1971.
[14] Skempton AW. The bearing capacity of clays. Building Research Congress, Division I, Part 3, London. 1951, p. 180–9.
[15] Bowles JE. Foundation analysis and design. 5th ed. New York, NY: McGraw-Hill; 1996.
[16] Evans LT. Simplified analysis of laterally loaded piles. PhD thesis, University of California, Berkeley, California. 1982, p. 211.
[17] SAP2000, Integrated finite element analysis and design of structures, Computers and Structures Inc., Berkeley, CA, 1998.
[18] FHWA, Seismic Design of Highway Bridge Foundations, Volume II: Design Procedures and Guidelines, Publication No. FHWA-RD-94-052, Federal Highway Administration, US Department of Transportation, Washington, DC, 1986.
[19] Burdette EG, Ingram EE, Goodpasture DW, Deatherage JH. Behavior of concrete integral abutments. Concrete International 2002;July:59–63.